Physiol Genomics
5: 171–179, 2001.

Cardiac remodeling and contractile function in acid α-glucosidase knockout mice

JOEP H. J. KAMPHOVEN,[1] RENE STUBENITSKY,[2] ARNOLD J. J. REUSER,[1] ANS T. VAN DER PLOEG,[3] PIETER D. VERDOUW,[2] AND DIRK J. DUNCKER[2]
[1]*Department of Clinical Genetics and* [2]*Experimental Cardiology, Thoraxcenter, Erasmus University Rotterdam, and* [3]*Department of Pediatrics, Sophia Children's Hospital Rotterdam, Rotterdam, The Netherlands*

Received 17 August 2000; accepted in final form 23 February 2001

Kamphoven, Joep H. J., Rene Stubenitsky, Arnold J. J. Reuser, Ans T. Van Der Ploeg, Pieter D. Verdouw, and Dirk J. Duncker. Cardiac remodeling and contractile function in acid α-glucosidase knockout mice. *Physiol Genomics* 5: 171–179, 2001.—Pompe's disease is an autosomal recessive and often fatal condition, caused by mutations in the acid α-glucosidase gene, leading to lysosomal glycogen storage in heart and skeletal muscle. We investigated the cardiac phenotype of an acid α-glucosidase knockout (KO) mouse model. Left ventricular weight-to-body weight ratios were increased 6.3 ± 0.8 mg/g in seven KO compared with 3.2 ± 0.2 mg/g in eight wild-type (WT) mice ($P < 0.05$). Echocardiography under ketamine-xylazine anesthesia revealed an increased left ventricular (LV) wall thickness (2.17 ± 0.16 in KO vs. 1.18 ± 0.10 mm in WT mice, $P < 0.05$) and a decreased LV lumen diameter (2.50 ± 0.32 in KO vs. 3.21 ± 0.14 mm in WT mice, $P < 0.05$), but LV diameter shortening was not different between KO and WT mice. The maximum rate of rise of left ventricular pressure (LV dP/dt_{max}) was lower in KO than in WT mice under basal conditions (2,720 ± 580 vs. 4,440 ± 440 mmHg/s) and during dobutamine infusion (6,220 ± 800 vs. 8,730 ± 790 mmHg/s, both $P < 0.05$). Similarly, during isoflurane anesthesia LV dP/dt_{max} was lower in KO than in WT mice under basal conditions (5,400 ± 670 vs. 8,250 ± 710 mmHg/s) and during norepinephrine infusion (10,010 ± 1,320 vs. 14,710 ± 220 mmHg/s, both $P < 0.05$). In conclusion, the markedly increased LV weight and wall thickness, the encroachment of the LV lumen, and LV dysfunction reflect cardiac abnormalities, although not as overt as in humans, of human infantile Pompe's disease and make these mice a suitable model for further investigation of pathophysiology and of novel therapies of Pompe's disease.

contractility; echocardiography; glycogen storage disease type II; lysosomal; metabolic disorder

POMPE'S DISEASE or glycogen storage disease type II (GSD II) is an autosomal recessive and often fatal disease caused by mutations in the acid α-glucosidase gene (16). The resultant deficiency of acid α-glucosidase activity prohibits degradation, and causes storage, of lysosomal glycogen in predominantly cardiac and skeletal muscle. Early and late onset forms of GSD II can be distinguished, which has been attributed to varying degrees of residual acid α-glucosidase activity (16, 24). The infantile form shows no residual activity, and patients suffering from this condition present themselves with hypotonia and hypertrophic cardiomegaly within a few months after birth. They usually die of cardiorespiratory failure before they reach the age of 1 yr (13, 24). Milder forms have residual activities up to 25% of normal values and are typically characterized by skeletal muscle weakness without involvement of the heart. Ultimately, these patients become wheelchair-bound and dependent on artificial ventilation.

Recently, knockout (KO) mouse models of GSD II have been developed (2–4, 22). In the present study, we investigated the cardiac phenotype of our mouse model, in terms of cardiac mass, left ventricular (LV) geometry, and LV contractile function and reserve to assess its usefulness for investigations into the pathophysiology of this disease and assessment of novel therapies.

METHODS

All experiments were conducted in accordance with the "Guiding Principles in the Care and Use of Animals" as approved by the American Physiological Society and with prior approval of the Animal Care Committee of the Erasmus University Rotterdam.

Experimental Design

In the first part of the study we investigated the LV morphological, geometrical, and contractile functional consequences of α-glucosidase deficiency in ketamine-xylazine anesthetized mice. To determine whether the low heart rates (250–300 beats/min) that were produced by ketamine-xylazine anesthesia influenced our results on LV contractile function, we repeated the hemodynamic measurements in the second part of the study in isoflurane-anesthetized mice, in which heart rates (450–600 beats/min) approximated the values we (450–550 beats/min; unpublished data from our laboratory) and others (478 ± 12 beats/min; Ref. 21) observe under awake conditions.

Article published online before print. See web site for date of publication (http://physiolgenomics.physiology.org).

Address for reprint requests and other correspondence: D. J. Duncker, Experimental Cardiology, Thoraxcenter, Erasmus Univ. Rotterdam, PO Box 1738, 3000 DR Rotterdam, The Netherlands (E-mail: Duncker@tch.fgg.eur.nl).

Experimental Groups

The acid α-glucosidase-deficient KO mice in this study were obtained by targeted disruption of the acid α-glucosidase gene in embryonic stem cells as previously described (2). For the first part of the study, we used seven KO mice of which three had been crossed back into FVB background for six generations and four into C57Bl/6 background for three generations. Eight wild-type (WT) littermates served as controls. Five of these were FVB, and three were C57Bl/6. FVB mice were between 10 and 14 mo of age, and C57Bl/6 mice were between 20 and 24 mo of age. For the second part of the study, we used three KO mice which had been crossed back into C57Bl/6 background for 10 generations, while 5 WT littermates served as controls. Mice were between 16 and 20 mo of age. The night before the experiment, mice were starved to deplete cytoplasmic glycogen (2, 4).

Experimental Protocol

Echocardiography. In the first part of the study, mice were weighed, anesthetized with ketamine (25 mg/kg ip) and xylazine (5 mg/kg ip), and hair from the left side of the thorax was shaved off. A tracheotomy was performed, a polyethylene tube (ID/OD, 0.58/0.80 mm) was inserted and secured with a suture to prevent leakage of air, and the mouse was artificially ventilated at a rate of 60–70 strokes/min (rodent ventilator; Harvard, Hilliston, MA). Electrocardiography (ECG) leads were connected, and the mouse was submerged in a water bath of 37°C, ~2 cm below the water surface. Echocardiograms were made with the HP Sonos 5500 echo device (Hewlett-Packard, Andover, MA) using a 12-MHz probe. Images of the short axis were obtained in 2D- and M-mode settings, with simultaneous recordings of ECG. All measurements were obtained while artificial ventilation was temporarily turned off.

Hemodynamic measurements. Following echocardiography, mice were removed from the water basin and placed on a heating pad. Body temperature was monitored via a rectal thermometer and maintained at 37°C. After receiving a second intraperitoneal bolus of anesthetics (25 mg/kg ketamine and 5 mg/kg xylazine) mice were instrumented for hemodynamic measurements. For this purpose, a polyethylene catheter (PE-10) was inserted into the right carotid artery and advanced into the aortic arch to measure aortic blood pressure. An identical catheter was introduced into the right external jugular vein and advanced into the superior caval vein for infusion of dobutamine. After a thoracotomy was performed through the 4th left intercostal space, the pericardium was opened and the heart was exposed. Subsequently, a 2-French Millar microtipped manometer (calibrated prior to each experiment with a mercury manometer) was inserted into the LV via the apex to measure LV pressure and its first derivative, LV dP/dt (obtained via electronic differentiation).

Following a 15-min stabilization period, baseline recordings were obtained of aortic blood pressure, heart rate, LV pressure, and LV dP/dt. A continuous intravenous infusion of dobutamine (concentration 10 μg/ml) was started at 2 $\mu g \cdot kg^{-1} \cdot min^{-1}$, and the rate of infusion was increased at 3-min intervals until LV dP/dt_{max} did not further increase. At peak responses to dobutamine all measurements were repeated.

Hemodynamic measurements under isoflurane anesthesia. In the second part of the study, mice were ventilated with a mixture of O_2 and N_2O (1/2, vol/vol) to which isoflurane (1.5–2.0 vol%) was added. The surgical instrumentation and experimental protocol were identical to that in the ketamine-xylazine anesthetized mice of the first part of the study, but we now used a 1.4-French Millar microtipped manometer to measure LV pressure. We observed in two pilot experiments in C57Bl/6 WT mice under isoflurane anesthesia that dobutamine produced a decrease in blood pressure, whereas it had no effect on heart rate, confirming previous observations by Hoit et al. (17). Therefore, we chose to infuse norepinephrine (concentration 20 μg/ml) starting at 2 $\mu g \cdot kg^{-1} \cdot min^{-1}$ iv and doubled the infusion rate every 3 min until LV dP/dt_{max} did not increase further.

Biochemistry and Morphology

At the conclusion of each experiment, the heart was excised and the atria were removed. The right ventricle (RV) and LV were separated, weighed, and freeze dried for the determination of dry weights and, in the first part of the study, for determination of acid α-glucosidase activity and glycogen content. In addition, samples were also obtained from the musculus quadriceps femoris and the liver to measure acid α-glucosidase activity and glycogen content. The atria and another sample from the musculus quadriceps femoris were fixed in glutaraldehyde (4%) and embedded in glycolmethacrylate, and histological sections of 4 μm were stained with hematoxylin azofloxin and periodic acid-Schiff. Tail DNA was extracted to verify the genotype by PCR (2).

Atria, muscle, and liver samples were homogenized in PBS, using an Ultra Turrax (TP18-10, 20,000 rpm; 170 W; see Ref. 2). Large debris was removed after centrifugation at 10,000 *g* for 15 min. The supernatant was sonicated on ice for two 10-s periods at an amplitude of 10 μm, then analyzed for total protein concentration with the bicinchoninic acid protein assay (BCA; Pierce, Rockford, IL) and acid α-glucosidase activity with 4-methylumbelliferyl-α-D-glucopyranoside (4MU) as substrate at a pH of 4.0. The glycogen content was measured after dialysis of the sample to remove cytoplasmic glucose, as previously described (2, 28).

Data Analysis

Echocardiography data were collected on an optical disk and stored for offline analysis. LV diameters at end-diastole (EDD) and end-systole (ESD) as well as the ED and ES thickness of the LV posterior wall were measured from the M-mode images using Clemex Vision software package (Clemex Technologies, Longueuil, Quebec, Canada). Five consecutive beats were analyzed in triplicate and averaged. LV absolute shortening (EDD − ESD) and fractional shortening [(EDD − ESD)/EDD × 100%] were calculated. Hemodynamic data were recorded and digitized using an online four-channel data acquisition program (ATCODAS; Dataq Instruments, Akron, OH) for postacquisition offline analysis with a program written in MATLAB (Mathworks, Natick, MA). Fifteen consecutive beats were selected for determination of heart rate, LV peak systolic and end-diastolic pressures, diastolic aortic pressure, and the maximum rates of rise (LVdP/dt_{max}) and fall (LVdP/dt_{min}) of LV pressure. In addition, the time constant (τ) of LV pressure decay, an index of early LV relaxation, was computed as described earlier (11).

Statistical analysis of anatomical and echocardiography data was performed using unpaired *t*-test or McNemar test as appropriate. Analysis of hemodynamic data was performed using two-way ANOVA followed by post hoc testing with paired and unpaired *t*-test or signed rank test and McNemar test, as appropriate. Statistical significance was accepted when $P < 0.05$ (two-tailed).

RESULTS

Biochemistry and Morphology

Biochemistry. The acid α-glucosidase activity in the heart of WT mice that were studied under ketamine-xylazine anesthesia was 12.6 ± 2.6 nmol 4MU·h^{-1}·mg protein^{-1} but only 1.0 ± 0.1 nmol 4MU·h^{-1}·mg protein^{-1} in KO mice. Consequently, the glycogen content in the heart was high in KO mice (330 ± 30 mg/ mg protein in 10- to 14-mo-old FVB KO mice, and 3,260 ± 980 mg/mg protein in 20- to 24-mo-old C57Bl/6 KO mice) and very low in WT mice (1.8 ± 0.9 mg/mg protein; Fig. 1).

Microscopy. Atria and skeletal muscle samples from all KO mice had periodic acid-Schiff-positive arrays of glycogen-filled lysosomes and lacework patterns resulting from lysosomal rupture and loss of content, as previously reported (4). Some of the WT mice showed little cytoplasmic glycogen content.

Macroscopy. The wet weight of the heart (HW) was on average 44% higher in KO compared with WT mice ($P < 0.05$), due to increases in both LV weight (LVW, 47%, $P < 0.05$) and RV weight (RVW, 31%, $P = 0.08$) (Table 1). Similar increments were observed in the dry weights of the whole heart, LV, and RV (all $P < 0.05$). Since total body weight (BW) was on average 30% lower in KO than in WT mice, it follows that the HW/BW, LVW/BW, and RVW/BW were almost doubled in KO compared with WT mice. KO mice with the highest glycogen content had the highest LVW/BW ratio (Fig. 1).

Echocardiography

The LV of KO mice was characterized by an increased wall thickness (83%, $P < 0.05$) and a modest encroachment of the LV lumen, reflected by an average 22% reduction in end-diastolic LV luminal diameter ($P < 0.05$) (Table 2). There were no significant differences between KO and WT mice in absolute (0.74 ± 0.05 vs. 0.99 ± 0.12 mm) or fractional (34 ± 3 vs. 30 ± 4%) LV diameter shortening. LV wall thickness showed a good correlation ($r^2 = 0.66$, $P < 0.01$) with the LVW/BW, whereas the LV lumen diameter did not correlate with LVW/BW (Fig. 2).

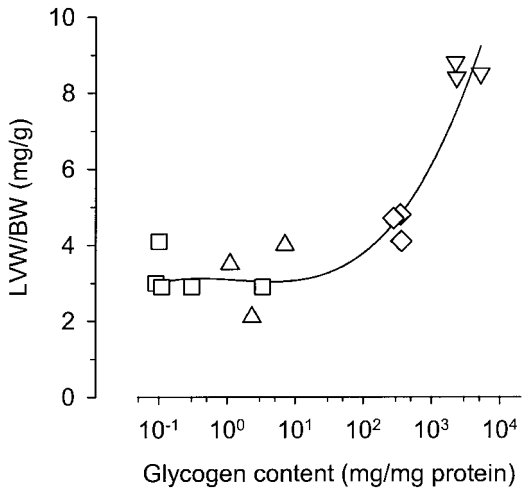

Fig. 1. Relation between left ventricular (LV) glycogen content and LV-to-body weight ratio (LVW/BW); □, 10- to 14-mo-old FVB wild-type (WT) mice; ◇, 10- to 14-mo-old FVB knockout (KO) mice; △, 20- to 24-mo-old C57Bl/6 WT mice; ▽, 20- to 24-mo-old C57Bl/6 KO mice.

Table 1. *Anatomic data*

	Wild-type Mice	Knockout Mice
n	8	7
BW, g	39 ± 3	29 ± 2*
HW, mg		
Wet	151 ± 11	217 ± 27*
Dry	37 ± 3	57 ± 7*
LVW, mg		
Wet	122 ± 10	179 ± 23*
Dry	30 ± 2	46 ± 6*
RVW, mg		
Wet	29 ± 2	38 ± 5†
Dry	7.5 ± 0.6	10.7 ± 1.2*
HW/BW, mg/g		
Wet	3.9 ± 0.3	7.6 ± 1.0*
Dry	0.96 ± 0.06	2.00 ± 0.26*
LVW/BW, mg/g		
Wet	3.2 ± 0.2	6.3 ± 0.8*
Dry	0.77 ± 0.05	1.63 ± 0.02*
RVW/BW, mg/g		
Wet	0.75 ± 0.04	1.32 ± 0.16*
Dry	0.19 ± 0.01	0.38 ± 0.05*

Values are means ± SE; *n* = number of observations. BW, body weight; HW, heart weight; LVW, left ventricular weight; RVW, right ventricular weight. *$P < 0.05$ vs. wild-type mice. †$P = 0.08$ vs. wild-type mice.

Hemodynamics

Baseline. Under baseline conditions, LV dP/dt_{max} and diastolic arterial pressure were lower in KO than in WT mice. The trends toward a lower heart rate, a lower diastolic arterial pressure, and a lower LV systolic pressure in KO mice and the trend toward the increase in τ in these mice did not reach levels of statistical significance (Table 3).

Pooling of all individual data points from KO and WT mice revealed an inverse correlation between LVW/BW and LV dP/dt_{max} ($r^2 = 0.76$), suggesting that LV contractility becomes more impaired with increased LVW (Fig. 3). However, since there was also an inverse correlation between LVW/BW and diastolic arterial pressure ($r^2 = 0.74$), the lower diastolic arterial pres-

Table 2. *Echocardiographic data*

	Wild-type Mice	Knockout Mice
n	8	7
LV-Th$_{ED}$, mm	1.18 ± 0.10	2.17 ± 0.16*
LV-Th$_{ES}$, mm	1.53 ± 0.06	2.39 ± 0.16*
LV-D$_{ED}$, mm	3.21 ± 0.14	2.50 ± 0.32*
LV-D$_{ES}$, mm	2.34 ± 0.22	1.59 ± 0.26*
Absolute LVD Shortening, mm	0.99 ± 0.12	0.74 ± 0.05
Fractional LVD Shortening, %	30 ± 4	34 ± 3

Values are means ± SE; *n* = number of observations. LV Th, left ventricular wall thickness; LV D, left ventricular lumen diameter. The subscripts ED and ES denote end diastole and end systole, respectively. *$P < 0.05$ vs. wild-type mice.

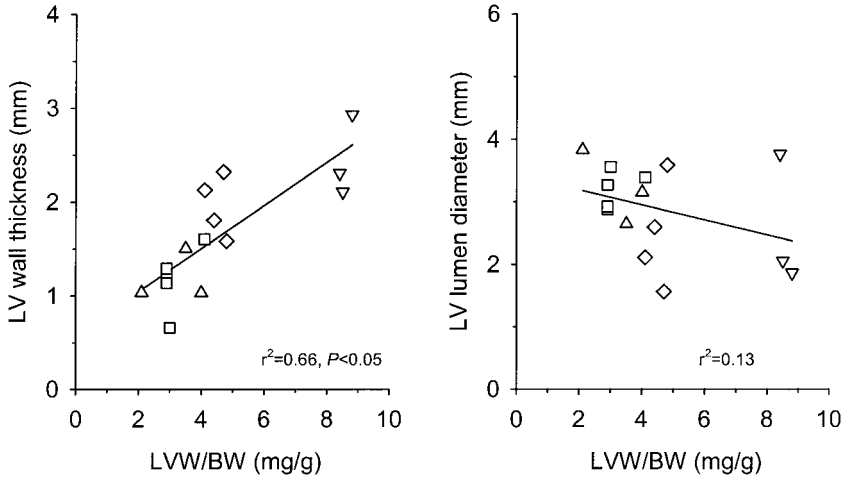

Fig. 2. Relation between LV wall thickness (*left*) and LV lumen diameter (*right*) and LVW/BW; symbols are the same as in Fig. 1.

sure in KO mice may have contributed to the lower LV dP/dt_{max} under basal conditions. Indeed, diastolic pressure and LV dP/dt_{max} were correlated ($r^2 = 0.76$, $P < 0.05$), and stepwise regression analysis revealed that diastolic arterial pressure was an independent predictor of LV dP/dt_{max} ($P < 0.05$). Similarly, there was a positive correlation between LVW/BW and LV dP/dt_{min} ($r^2 = 0.85$), but also between LVW/BW and LV systolic pressure ($r^2 = 0.76$). The lower LV systolic pressure may have contributed to the lower maximum rate of fall of LV pressure, as is suggested by the close correlation between LV systolic pressure and LV dP/dt_{min} observed during univariate regression analysis ($r^2 = 0.96$, $P < 0.05$). In addition, stepwise regression analysis showed LV systolic pressure to be an independent determinant of LV dP/dt_{min} ($P < 0.05$). The time constant τ, which describes the rate of relaxation during early diastole, was considerably higher in KO mice with the highest LVW/BW, suggesting impaired LV relaxation in these mice (Fig. 3). In contrast, LV end-diastolic pressures were not increased in KO compared with WT mice.

Table 3. *Hemodynamic data during ketamine-xylazine anesthesia*

	Wild-type Mice	Knockout Mice
n	6	6
HR, beats/min		
Baseline	308 ± 28	234 ± 19
Dobutamine	475 ± 37†	401 ± 25†
DAP, mmHg		
Baseline	60 ± 3	42 ± 7*
Dobutamine	69 ± 8	50 ± 7
LVSP, mmHg		
Baseline	83 ± 4	65 ± 8
Dobutamine	109 ± 9†	117 ± 15†
LVEDP, mmHg		
Baseline	9 ± 1	6 ± 1*
Dobutamine	9 ± 2	3 ± 2*
LV dP/dt_{max}, mmHg/s		
Baseline	4,440 ± 440	2,720 ± 580*
Dobutamine	8,730 ± 790†	6,220 ± 800*†
LV dP/dt_{min}, mmHg/s		
Baseline	−3,290 ± 190	−2,110 ± 500*
Dobutamine	−5,960 ± 530†	−4,730 ± 350†
τ, ms		
Baseline	18.6 ± 1.1	71.4 ± 46.2
Dobutamine	13.7 ± 0.5†	13.4 ± 0.6†

Values are means ± SE; *n* = number of observations. HR, heart rate; DAP, diastolic arterial blood pressure; LVSP, left ventricular systolic blood pressure; LVEDP, left ventricular end diastolic blood pressure; LV dP/dt_{max}, maximum rate of rise of left ventricular pressure; LV dP/dt_{min}, maximum rate of fall of LV pressure; τ, time constant of early diastolic LV pressure decay. *$P < 0.05$ vs. wild-type mice. †$P < 0.05$ vs. baseline.

Dobutamine. Intravenous infusion of dobutamine increased heart rate, diastolic arterial pressure, LV systolic pressure, LV dP/dt_{max}, and LV dP/dt_{min}, and decreased τ, but had no effect on LV end-diastolic pressure in both WT and KO mice (Table 3). There were no differences in the responses to dobutamine in KO and WT mice. During dobutamine infusion, the inverse correlation between LVW/BW and LV dP/dt_{max} was maintained ($r^2 = 0.62$), but the inverse correlation between LVW/BW and diastolic arterial pressure was not significant (Fig. 3), indicating that the lower LV dP/dt_{max} during dobutamine was principally the result of a lower global LV contractility. During dobutamine infusion, the relation between LVW/BW and LV dP/dt_{min} was maintained, but τ was no longer different in KO and WT mice. The doses of dobutamine needed to produce maximal increases in LV dP/dt_{max} in KO and WT mice were 9 ± 2 and 8 ± 2 $\mu g \cdot kg^{-1} \cdot min^{-1}$, respectively.

Hemodynamics During Isoflurane Anesthesia

Baseline hemodynamics. Heart rate and LV dP/dt_{max} were significantly higher during isoflurane anesthesia (Table 4) than during ketamine-xylazine anesthesia (Table 3). Despite these differences in hemodynamics produced by the two anesthesia regimens, heart rate (471 ± 28 vs. 581 ± 23 beats/min) and LV dP/dt_{max} (5,400 ± 670 vs. 8,250 ± 710 mmHg/s) were again lower in KO than in WT mice (both $P < 0.05$), whereas diastolic arterial blood pressure (64 ± 6 vs. 58 ± 5 mmHg) and LV systolic pressure (94 ± 10 vs. 122 ± 14 mmHg) were not different. In these animals, ratios of HR/BW, LVW/BW, and RVW/BW were, respectively,

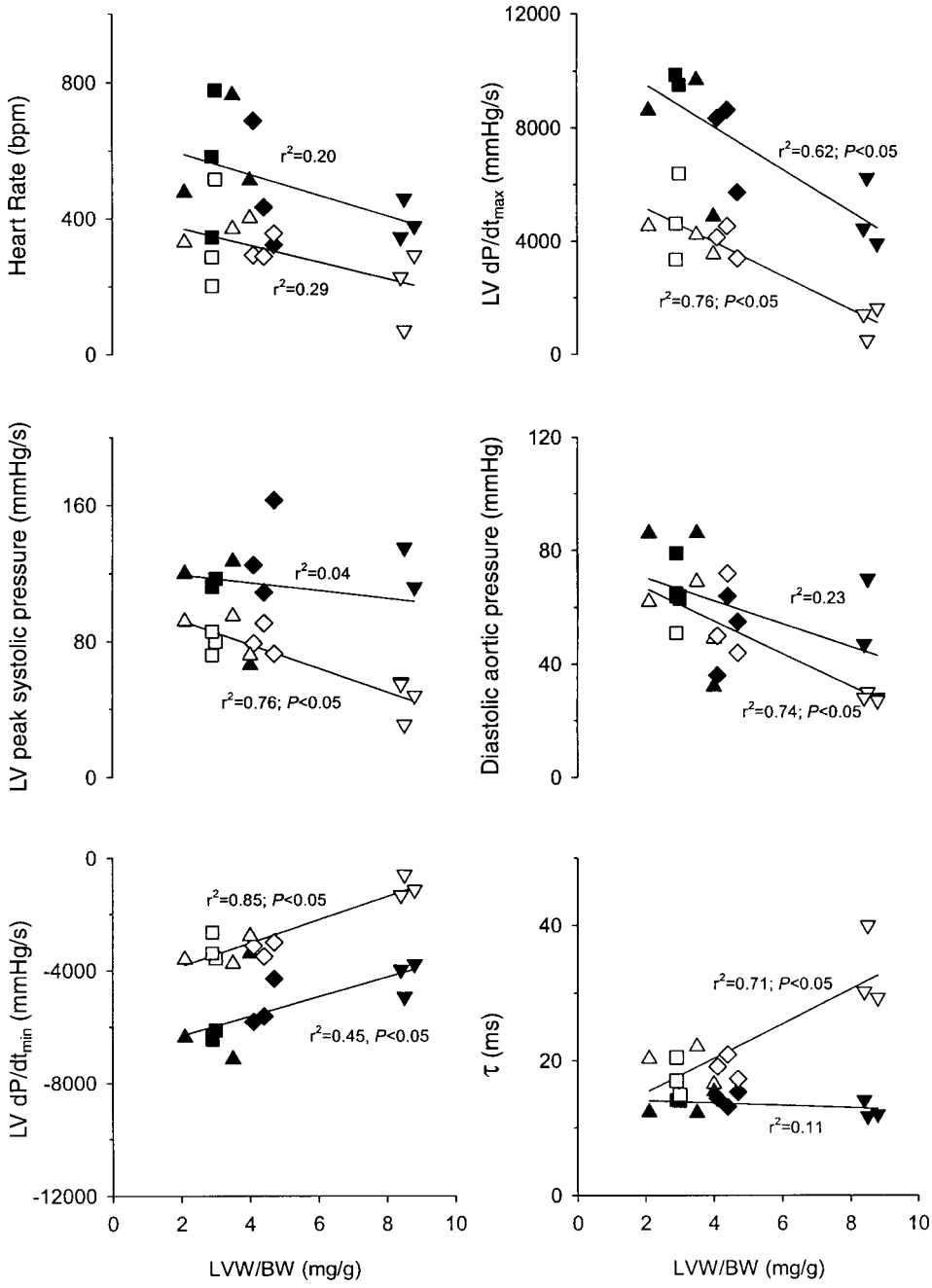

Fig. 3. Relation between hemodynamic variables under control conditions (open symbols) and during intravenous dobutamine infusion (solid symbols) and LVW/BW, in ketamine-xylazine anesthetized mice; otherwise, symbols are the same as in Fig. 1.

94% (8.00 ± 0.47 in KO mice vs. 4.12 ± 0.19 mg/g in WT mice), 98% (6.43 ± 0.40 vs. 3.25 ± 0.16 mg/g), and 80% (1.57 ± 0.08 vs. 0.87 ± 0.05 mg/g) higher in the C57Bl/6 KO mice at 16–18 mo of age than in WT littermates.

Similar to the study under ketamine-xylazine anesthesia, there were correlations between LVW/BW and LV dP/dt_{max} ($r^2 = 0.79$), LVW/BW and LV dP/dt_{min} ($r^2 = 0.52$), and LVW/BW and τ ($r^2 = 0.52$; all $P < 0.05$) in the isoflurane-anesthetized mice (Fig. 4). There was also an inverse correlation between LVW/BW and heart rate ($r^2 = 0.61$), suggesting that the lower heart rate in KO mice may have contributed to the aforementioned correlations. Univariate regression analysis showed a correlation between heart rate and LV dP/dt_{max} ($r^2 = 0.36$, $P = 0.07$) and τ ($r^2 = 0.47$, $P < 0.05$), but not LV dP/dt_{min} ($r^2 = 0.10$), under basal conditions. However, stepwise regression analysis showed that heart rate did not contribute significantly to the prediction of LV dP/dt_{max} ($P = 0.55$), LV dP/dt_{min} ($P = 0.48$), or τ ($P = 0.27$), in addition to LVW/BW.

Norepinephrine. Intravenous infusion of norepinephrine increased heart rate, diastolic arterial pressure, LV systolic pressure, and LV dP/dt_{max} in both WT and KO mice (Table 4). There were no significant differences in the responses to norepinephrine in KO and WT mice, with the exception of heart rate which increased only in the KO mice, so that heart rates were

Table 4. *Hemodynamic data during isoflurane anesthesia*

	Wild-type Mice	Knockout Mice
n	5	3
HR, beats/min		
Baseline	581 ± 23	471 ± 28*
Norepinephrine	557 ± 10†	543 ± 12‡
DAP, mmHg		
Baseline	58 ± 5	64 ± 6
Norepinephrine	96 ± 10†	92 ± 3‡
LVSP, mmHg		
Baseline	120 ± 14	94 ± 10
Norepinephrine	191 ± 11†	147 ± 26‡
LVEDP, mmHg		
Baseline	10 ± 1	8 ± 1
Norepinephrine	10 ± 1	9 ± 1
LV dP/dt_{max}, mmHg/s		
Baseline	8,250 ± 710	5,400 ± 670*
Norepinephrine	14,710 ± 220†	10,010 ± 1,320*‡
LV dP/dt_{min}, mmHg/s		
Baseline	−9,260 ± 1,270	−4,420 ± 860*
Norepinephrine	−12,200 ± 810†	−7,630 ± 1,120*‡
τ, ms		
Baseline	10.5 ± 1.3	16.5 ± 1.6*
Norepinephrine	8.4 ± 1.0†	10.3 ± 1.0‡

Values are means ± SE; *n* = number of observations. HR, heart rate; DAP, diastolic arterial blood pressure; LVSP, left ventricular systolic blood pressure; LVEDP, left ventricular end diastolic blood pressure; LV dP/dt_{max}, maximum rate of rise of left ventricular pressure; LV dP/dt_{min}, maximum rate of fall of LV pressure; τ, time constant of early diastolic LV pressure decay. *$P < 0.05$ vs. wild-type mice. †$P < 0.05$ vs. baseline. ‡Variable increased or decreased in all three knockout mice.

no longer different in KO and WT mice. During norepinephrine infusion, the inverse correlation between LVW/BW and LV dP/dt_{max} became even more pronounced ($r^2 = 0.62$), in the absence of a significant relation between LVW/BW and heart rate, diastolic arterial pressure, or LV systolic pressure (Fig. 4), indicating that the lower LV dP/dt_{max} during norepinephrine was principally the result of a lower global LV contractility. During norepinephrine infusion, the relation between LVW/BW and LV dP/dt_{min} was maintained. Similar to the ketamine-xylazine study, τ was again no longer different in KO and WT mice during norepinephrine infusion. The doses of norepinephrine needed to produce the maximal responses in LV dP/dt_{max} in KO and WT mice were 11 ± 3 and 11 ± 2 $\mu g \cdot kg^{-1} \cdot min^{-1}$, respectively.

DISCUSSION

The major findings of the present study are that *1*) mice lacking acid α-glucosidase activity show an increase in cardiac mass involving both LV and RV, *2*) the increase in LVW is associated with a marked increase in LV wall thickness and encroachment of the LV lumen, and *3*) the degree of LV mass increase is inversely correlated with the loss of maximal attainable LV global contractility during β-adrenergic stimulation.

Cardiac Mass

Qualitative descriptions of enlarged hearts have been previously reported in naturally occurring GSD II in turkey (9), sheep (19), dog (29), and a subpopulation of shorthorn cattle (18). HW, LVW, and RVW were reported in only one study in two calves, at an age of 3–7 mo, in which the HW/BW ratio had tripled compared with normal, due to more than a doubling of LVW and a quadrupling of RVW (25). In the present murine study, we observed an increase in relative heart weight (HW) of up to 160%, due to a 166% increase in relative LVW and a 130% increase in relative RVW. We observed a strong correlation between glycogen storage in the heart and the relative LVW. In ~10- to 14-mo-old FVB KO mice, the average glycogen content was around 300 mg/mg protein, whereas in 20- to 24-mo-old C57Bl/6 KO mice glycogen content was between 2,200 and 5,200 mg/mg protein, resulting in a 40% increase in relative LVW in 10- to 14-mo-old FVB and a 166% increase in 20- to 24-mo-old C57Bl/6 KO mice. In the three additional 16- to 18-mo-old C57Bl/6 KO mice, relative LVW was 98% higher than in littermate WT mice. Together, these findings suggest that glycogen continues to accumulate in the murine heart up to 2 yr of age. The increase in relative HW in mice (up to 160% at 24 mo + 3 wk gestation time) approximates that in calves (up to 200% at 3.7 mo + 6 mo gestation time), but is significantly less than the increase in humans (up to 350% at 3–10 mo + 9 mo gestation time). Interestingly, the increase in relative HW in humans appears to level off after ~3 mo after birth, as HWs are ~3 times normal at 2 wk of age ($n = 8$) and 4.5 times normal at 3 mo ($n = 8$), but with no significant further increase between 3 and 10 mo ($n = 40$) (1, 8, 12, 20). In contrast, glycogen continues to accumulate in the murine heart between 10 mo and 24 mo of age.

LV Wall Thickness and Lumen Diameter

Data on alterations in LV geometry in infants with GSD II have been obtained during autopsy and revealed increases in wall thickness of 6–10 mm in the LV (normal range 2–4 mm) a few weeks after birth, whereas in children who died at ~2 yr of age, wall thickness had increased up to a maximum of 25 mm in the LV (normal range 4–6 mm) (12). More recent echocardiography studies have generally reported severe cardiomegaly with extremely thick ventricular walls and relatively normal atria (7). In most cases hypertrophy of the LV free wall and septum is more pronounced than in the RV (14). Another typical echocardiography finding is the encroachment of the LV lumen as was found in two girls of 6–7 mo of age (14, 23). Encroachment of the lumen may become so severe that outflow tract obstruction and inflow impairment develop (12, 23, 27).

The present study is the first to describe the echocardiography abnormalities in an animal model of GSD II. The main feature of the echocardiography findings was an increased LV wall thickness up to 200% of WT mice together with a modest encroachment of the LV lumen, which corresponds well with the echocardiography findings in infantile GSD II in humans. The degree of encroachment was somewhat variable and did not occur in all KO animals (Fig. 1) but could reflect the onset of LV failure with resulting LV dilation.

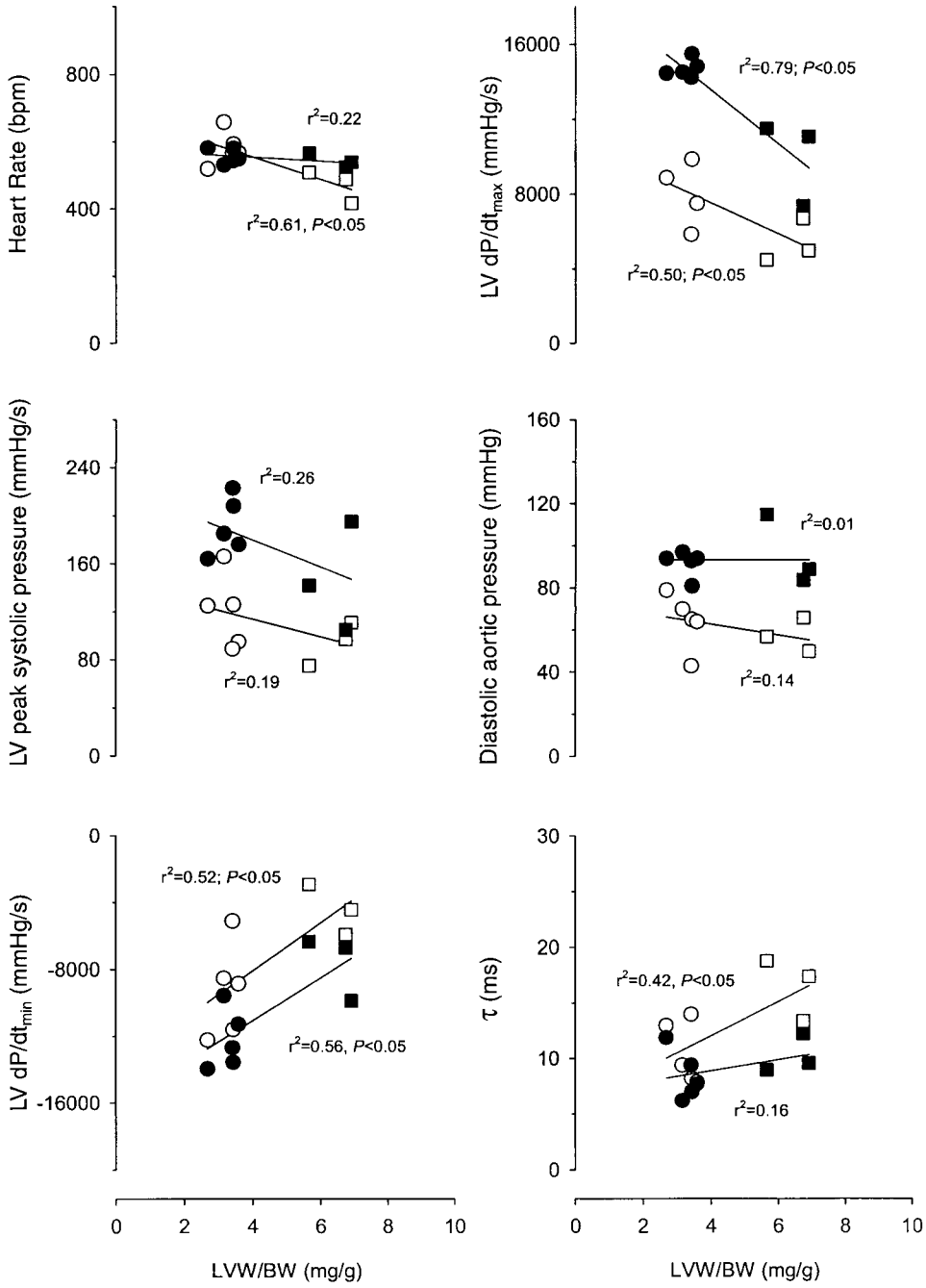

Fig. 4. Relation between hemodynamic variables under control conditions (open symbols) and during intravenous norepinephrine infusion (solid symbols) and LVW/BW in isoflurane anesthetized mice; circles, 16- to 20-mo-old C57Bl/6 WT mice; squares, 16- to 20-mo-old C57Bl/6 KO mice.

LV Contractile Function and Reserve

In contrast to the well-described anatomic and echocardiography abnormalities in patients with GSD II, there is surprisingly little information on LV contractile function in GSD II. De Dominicis et al. (10) reported normal ejection fractions (70% and 68%) measured with echocardiography in two 6-mo-old patients. Bulkley and Hutchins (7) also reported a normal ejection fraction (>70%), measured with LV angiography, in a 5-mo-old girl. In two other case reports (children up to 9 mo of age), invasive assessment of LV function using cardiac catheterization demonstrated normal LV filling pressures (2–3 mmHg), in the presence of severe cardiomegaly (12, 15). In another case report (4 mo of age) normal LV hemodynamics and cardiac index were observed, although early diastolic pressure was elevated with a restrictive LV filling pattern (5). In contrast, markedly elevated LV filling pressures (up to 20 mmHg) and a depressed cardiac index (2.44 $l \cdot min^{-1} \cdot m^{-2}$) were found in a 4-mo-old child (26). In all these case studies, children invariably developed progressive clinical heart failure and died within 2 mo after catheterization. Unfortunately, in none of these studies were LV contractility and LV contractile reserve determined.

The present murine study also shows a normal fractional LV diameter shortening in KO compared with WT mice under basal conditions. However, LV function

was not normal, as we observed decreases in LV dP/dt_{max}, under basal conditions and, in particular, during β-adrenergic stimulation with either dobutamine or norepinephrine infusion. The additional experiments with norepinephrine were performed during isoflurane anesthesia to exclude that the low heart rates and LV dP/dt_{max} values observed during ketamine-xylazine anesthesia influenced the results (21). In addition, we used a 1.4-French microtipped manometer in these experiments to further minimize mechanical perturbation of LV volume and contractile performance. The maximal attainable LV dP/dt_{max} correlated well with the increase in LVW in both series of experiments, thus independent of the anesthesia regimen or size of the LV catheter, suggesting that at more severe stages of the disease LV function becomes impaired. However, from the present study it also becomes clear that the KO animals are not yet in severe cardiac failure. This is suggested by the normal fractional LV diameter shortening and by the comparable doses of both dobutamine and norepinephrine needed to elicit maximal responses of LV dP/dt_{max} in KO compared with WT mice, suggesting normal β-adrenergic receptor sensitivity (6). Moreover, although the less negative LV dP/dt_{min} and increase in τ in KO compared with WT mice indicate a slight impairment of early diastolic function, which is in close agreement with human data (5), the normal levels of LV filling pressure in KO compared with WT mice also suggest the absence of overt diastolic dysfunction.

Conclusions

The present study demonstrates that the acid α-glucosidase KO mouse model is characterized by increased cardiac mass, which is associated with an increased LV free wall thickness and with encroachment of the LV lumen, as well as a lower global LV contractility. These manifestations of cardiomegaly and LV dysfunction, although not as overt, parallel the human conditions of early onset GSD II and make these mice a suitable model for further investigation of pathophysiology and novel therapies of infantile Pompe's disease.

We gratefully acknowledge the technical assistance of Elza D. van Deel and Monique C. de Waard.

This study was in part financed by a grant from the Sophia Foundation for Medical Research. D. J. Duncker was supported by a Research Fellowship of the Royal Netherlands Academy of Arts and Sciences and by an Established Investigator Grant of the Netherlands Heart Foundation (2000D038).

REFERENCES

1. **Bharati S, Serratto M, DuBrow I, Paul MH, Swiryn S, Miller RA, Rosen K, and Lev M.** The conduction system in Pompe's disease. *Pediatr Cardiol* 2: 25–32, 1982.
2. **Bijvoet AG, Van de Kamp EH, Kroos MA, Ding JH, Yang BZ, Visser P, Bakker CE, Verbeet MP, Oostra BA, Reuser AJ, and Van der Ploeg AT.** Generalized glycogen storage and cardiomegaly in a knockout mouse model of Pompe disease. *Hum Mol Genet* 7: 53–62, 1998.
3. **Bijvoet AG, Van Hirtum H, Kroos MA, Van de Kamp EH, Schoneveld O, Visser P, Brakenhoff JP, Weggeman M, Van Corven EJ, Van der Ploeg AT, and Reuser AJJ.** Human acid alpha-glucosidase from rabbit milk has therapeutic effect in mice with glycogen storage disease type II. *Hum Mol Genet* 8: 2145–2153, 1999.
4. **Bijvoet AG, Van Hirtum H, Vermey M, Van Leenen D, Van der Ploeg AT, Mooi WJ, and Reuser AJJ.** Pathological features of glycogen storage disease type II highlighted in the knockout mouse model. *J Pathol* 189: 416–424, 1999.
5. **Bonnici F, Shapiro R, Joffe HS, and Petersen EM.** Angiocardiographic and enzyme studies in a patient with type II glycogenosis (Pompe's disease). A case report. *S Afr Med J* 58: 860–862, 1980.
6. **Bristow MR, Ginsburg R, Minobe W, Cubicciotti RS, Sageman WS, Lurie K, Billingham ME, Harrison C, and Stinson EB.** Decreased catecholamine sensitivity and beta-adrenergic-receptor density in failing human hearts. *N Engl J Med* 307: 205–211, 1982.
7. **Bulkley BH and Hutchins GM.** Pompe's disease presenting as hypertrophic myocardiopathy with Wolff-Parkinson-White syndrome. *Am Heart J* 96: 246–252, 1978.
8. **Childs AW, Grose RF, and Henderson PH.** Glycogen disease of the heart. Report of two cases occurring in siblings. *Pediatrics* 10: 208–217, 1952.
9. **Czarnecki CM, Reneau JK, and Jankus EF.** Blood glucose and tissue glycogen levels in turkey poults with spontaneous round heart disease and furazolidone-induced cardiomyopathy. *Avian Dis* 19: 773–780, 1975.
10. **De Dominicis E, Finocchi G, Vincenzi M, Calvelli M, Ronconi G, Angelini C, and Vergani L.** Echocardiographic and pulsed Doppler features in glycogen storage disease type II of the heart (Pompe's disease). *Acta Cardiol* 46: 107–114, 1991.
11. **De Zeeuw S, Trines SA, Krams R, Verdouw PD, and Duncker DJ.** Cardiovascular profile of the calcium sensitizer EMD 57033 in open-chest anaesthetized pigs with regionally stunned myocardium. *Br J Pharmacol* 129: 1413–1422, 2000.
12. **Ehlers KH, Hagstrom JWC, Lukas DS, Redo SF, and Engele MA.** Glycogen-storage disease of the myocardium with obstruction to the left ventricular outflow. *Circulation* 25: 96–108, 1962.
13. **Engel AG, Gomez MR, Seybold ME, and Lambert EH.** The spectrum and diagnosis of acid maltase deficiency. *Neurology* 23: 95–106, 1973.
14. **Gussenhoven WJ, Busch HF, Kleijer WJ, and De Villeneuve VH.** Echocardiographic features in the cardiac type of glycogen storage disease II. *Eur Heart J* 4: 41–43, 1983.
15. **Hernandez A Jr, Marchesi V, Goldring D, Kissane J, and Hartmann AF Jr.** Cardiac glycogenosis. Hemodynamic, angiocardiographic, and electron microscopic findings-report of a case. *J Pediatr* 68: 400–412, 1966.
16. **Hirschhorn R and Reuser AJJ.** Glycogen storage disease type II: acid α-glucosidase (acid maltase) deficiency. In: *The Metabolic and Molecular Bases of Inherited Disease*, edited by Scriver CR, Beaudet AL, Valle D, and Sly WS. New York: McGraw-Hill, 2001, p. 3389–3420.
17. **Hoit BD, Khan ZU, Pawloski-Dahm CM, and Walsh RA.** In vivo determination of left ventricular wall stress-shortening relationship in normal mice. *Am J Physiol Heart Circ Physiol* 272: H1047–H1052, 1997.
18. **Howell JM, Dorling PR, Cook RD, Robinson WF, Bradley S, and Gawthorne JM.** Infantile and late onset form of generalised glycogenosis type II in cattle. *J Pathol* 134: 267–277, 1981.
19. **Manktelow BW and Hartley WJ.** Generalized glycogen storage disease in sheep. *J Comp Pathol* 85: 139–145, 1975.
20. **Nihill MR, Wilson DS, and Hugh-Jones K.** Generalized glycogenosis type II (Pompe's disease). *Arch Dis Child* 45: 122–129, 1970.
21. **Palakodeti V, Oh S, Oh BH, Mao L, Hongo M, Peterson KL, and Ross J.** Force-frequency effect is a powerful determinant of myocardial contractility in the mouse. *Am J Physiol Heart Circ Physiol* 273: H1283–H1290, 1997.
22. **Raben N, Nagaraju K, Lee E, Kessler P, Byrne B, Lee L, LaMarca M, King C, Ward J, Sauer B, and Plotz P.** Targeted disruption of the acid α-glucosidase gene in mice causes an illness with critical features of both infantile and adult human glycogen storage disease type II. *J Biol Chem* 273: 19086–19092, 1998.

23. **Rees A, Elbl F, Minhas K, and Solinger R.** Echocardiographic evidence of outflow tract obstruction in Pompe's disease (glycogen storage disease of the heart). *Am J Cardiol* 37: 1103–1106, 1976.
24. **Reuser AJ, Kroos MA, Hermans MM, Bijvoet AG, Verbeet MP, van Diggelen OP, Kleijer WJ, and van der Ploeg AT.** Glycogenosis type II (acid maltase deficiency). *Muscle Nerve* 3: S61–S69, 1995.
25. **Robinson WF, Howell JM, and Dorling PR.** Cardiomyopathy in generalised glycogenosis type II in cattle. *Cardiovasc Res* 17: 238–242, 1983.
26. **Ruttenberg HD, Steidl RM, Carey LS, and Edwards JE.** Glycogen-storage disease of the heart. Hemodynamic and angiocardiographic features in 2 cases. *Am Heart J* 67: 469–480, 1964.
27. **Seifert BL, Snyder MS, Klein AA, O'Loughlin JE, Magid MS, and Engle MA.** Development of obstruction to ventricular outflow and impairment of inflow in glycogen storage disease of the heart: serial echocardiographic studies from birth to death at 6 months. *Am Heart J* 123: 239–242, 1992.
28. **Van der Ploeg AT, Kroos M, van Dongen JM, Visser WJ, Bolhuis PA, Loonen MC, and Reuser AJJ.** Breakdown of lysosomal glycogen in cultured fibroblasts from glycogenosis type II patients after uptake of acid α-glucosidase. *J Neurol Sci* 79: 327–336, 1987.
29. **Walvoort HC, Slee RG, and Koster JF.** Canine glycogen storage disease type II. A biochemical study of an acid alpha-glucosidase-deficient Lapland dog. *Biochim Biophys Acta* 715: 63–69, 1982.